cmgh
CELLULAR AND MOLECULAR GASTROENTEROLOGY AND HEPATOLOGY

ORIGINAL RESEARCH

THBS2 Is a Candidate Modifier of Liver Disease Severity in Alagille Syndrome

Ellen A. Tsai,[1,2,*] Melissa A. Gilbert,[1,*] Christopher M. Grochowski,[1] Lara A. Underkoffler,[1] He Meng,[3] Xiaojie Zhang,[3] Michael M. Wang,[3,4,5] Hailu Shitaye,[6] Kurt D. Hankenson,[7,8] David Piccoli,[9] Henry Lin,[9] Binita M. Kamath,[10] Marcella Devoto,[11,12,13] Nancy B. Spinner,[1] and Kathleen M. Loomes[9]

[1]*Department of Pathology and Laboratory Medicine,* [9]*Division of Pediatric Gastroenterology, Hepatology, and Nutrition,* [11]*Division of Genetics, Department of Pediatrics, Children's Hospital of Philadelphia,* [2]*Genomics and Computational Biology Graduate Group,* [8]*Department of Orthopaedic Surgery,* [12]*Department of Biostatistics and Epidemiology, Perelman School of Medicine, University of Pennsylvania, Philadelphia, Pennsylvania;* [3]*Department of Neurology,* [4]*Department of Physiology,* [6]*Medical Scientist Training Program, University of Michigan, Ann Arbor, Michigan;* [5]*VA Ann Arbor Healthcare System, Ann Arbor, Michigan;* [7]*Department of Physiology, Department of Small Animal Clinical Sciences, Colleges of Natural Science, Osteopathic Medicine, and Veterinary Medicine, Michigan State University, East Lansing, Michigan;* [10]*Division of Gastroenterology, Hepatology, and Nutrition, Hospital for Sick Children, University of Toronto, Toronto, Canada;* [13]*Department of Molecular Medicine, University La Sapienza, Rome, Italy*

SUMMARY

THBS2, identified in this genome-wide association study, is expressed in mouse bile ducts, and the protein appears to inhibit JAG1–NOTCH2 interactions. These data implicate *THBS2* as a candidate genetic modifier of liver disease severity in Alagille syndrome.

BACKGROUND & AIMS: Alagille syndrome is an autosomal-dominant, multisystem disorder caused primarily by mutations in *JAG1*, resulting in bile duct paucity, cholestasis, cardiac disease, and other features. Liver disease severity in Alagille syndrome is highly variable, however, factors influencing the hepatic phenotype are unknown. We hypothesized that genetic modifiers may contribute to the variable expressivity of this disorder.

METHODS: We performed a genome-wide association study in a cohort of Caucasian subjects with known pathogenic *JAG1* mutations, comparing patients with mild vs severe liver disease, followed by functional characterization of a candidate locus.

RESULTS: We identified a locus that reached suggestive genome-level significance upstream of the thrombospondin 2 (*THBS2*) gene. *THBS2* codes for a secreted matricellular protein that regulates cell proliferation, apoptosis, and angiogenesis, and has been shown to affect Notch signaling. By using a reporter mouse line, we detected thrombospondin 2 expression in bile ducts and periportal regions of the mouse liver. Examination of *Thbs2*-null mouse livers showed increased microvessels in the portal regions of adult mice. We also showed that thrombospondin 2 interacts with NOTCH1 and NOTCH2 and can inhibit JAG1–NOTCH2 interactions.

CONCLUSIONS: Based on the genome-wide association study results, thrombospondin 2 localization within bile ducts, and demonstration of interactions of thrombospondin 2 with JAG1 and NOTCH2, we propose that changes in thrombospondin 2 expression may further perturb JAG1–NOTCH2 signaling in patients harboring a *JAG1* mutation and lead to a more severe liver phenotype. These results implicate *THBS2* as a plausible candidate genetic modifier of liver disease severity in Alagille syndrome. *(Cell Mol Gastroenterol Hepatol 2016;2:663–675; http://dx.doi.org/10.1016/j.jcmgh.2016.05.013)*

Keywords: JAG1; NOTCH2; Gene Modifier; Cholestasis; Genome-Wide Association Study.

Alagille syndrome (ALGS) is an autosomal-dominant disorder caused by mutations in the Notch pathway ligand *JAG1* in 94% of patients and in 1 of 4 Notch receptors (*NOTCH2*) in 1%–2%. ALGS is characterized by bile duct paucity, cholestatic liver disease, congenital heart lesions, eye and skeletal anomalies, and a characteristic facial appearance. However, there is extensive variation in the expressivity of the disease, and variable penetrance of clinical features in ALGS patients has been observed since the earliest description of the syndrome.[1] Before mutations in *JAG1* were found to be the principal cause of ALGS, examination of inherited cases showed extreme phenotypic variability, even among family members.[2-4] We suspect that this phenotypic

*Authors share co-first authorship.

Abbreviations used in this paper: **ALGS, Alagille syndrome; BSA, bovine serum albumin; cDNA, complementary DNA; ChiLDReN, Childhood Liver Disease Research Network; CK19, cytokeratin 19; ddPCR, droplet digital polymerase chain reaction; GFP, green fluorescent protein; GWAS, genome-wide association study; PCR, polymerase chain reaction; SNP, single-nucleotide polymorphism; THBS2, thrombospondin 2.**

Most current article

2352-345X
http://dx.doi.org/10.1016/j.jcmgh.2016.05.013

variability, including liver disease severity, is associated with genetic modifiers.

The liver disease seen in ALGS patients is highly variable, ranging from subclinical to severe, and factors influencing the hepatic phenotype are unknown. Unlike the cardiac defects, in which severe forms of cardiac disease can be categorized at initial presentation, liver disease severity cannot be predicted based on the presence of bile duct paucity alone. Early symptoms may resolve and never develop into severe liver disease, however 20%–30% of ALGS patients eventually will require liver transplantation.[5–8] It also has been observed that liver disease in children younger than 5 years of age is not a stable predictor of long-term need for liver transplantation,[9] although more recent work has shown that the combinatorial quantification of serum total bilirubin, liver biopsy fibrosis, and the presence of xanthomata is predictive of long-term hepatic disease, offering a prognostic metric for this phenotype.[10] No environmental factor influencing liver disease severity has been identified to date. Attempts to establish a genotype–phenotype correlation between *JAG1* mutations and the liver phenotype have been unable to substantiate any connection,[11–14] and there presently is no reliable genetic biomarker that is able to explain the high degree of liver disease variability seen in ALGS. We hypothesize that genetic modifying factors contribute to this phenotype, such that some children will progress to end-stage liver disease because of their genetic risk.

We designed a genome-wide association study (GWAS) to identify loci that influence liver disease severity in ALGS patients. The strongest association was found in the genomic region upstream of the gene encoding thrombospondin 2, a matricellular protein known to interact with the Notch signaling pathway.

Materials and Methods

Sample Cohort and Stratification

ALGS patients who were positive for a *JAG1* mutation were enrolled in the study either through the Children's Hospital of Philadelphia or through the Longitudinal Study of Genetic Causes of Intrahepatic Cholestasis protocol within the Childhood Liver Disease Research Network (ChiLDReN), a National Institute of Diabetes and Digestive and Kidney Diseases/National Institutes of Health–funded network of 16 pediatric academic medical centers across North America. This study was approved by the Institutional Review Boards at each center and informed consent was obtained from parents/guardians or subjects 18 years or older. Data from all patients were reviewed to determine liver disease severity, using a stratification protocol based on a combination of clinical and biochemical findings (Table 1). At the time of enrollment in this study, there was no reliable predictor of outcome before age 5, therefore stratification was limited to ALGS patients older than 5 years of age.[9] The 2 cohorts, mild and severe, showed no correlation in *JAG1* mutation type, as has been reported previously (Supplementary Table 1).[11–14]

Table 1. Stratification of Liver Disease Severity

Liver disease severity	Clinical features
Mild	1. No known hepatic involvement; normal liver test results 2. Biochemical abnormalities (serum aminotransferase levels greater than the upper limit of normal for the laboratory, but not normal bilirubin) 3. Biochemical cholestasis without overt clinical manifestations: increased conjugated bilirubin (>15% of total bilirubin or >2 mg/dL) or increased cholesterol, bile salts, or γ-glutamyltransferase levels above the upper limit of normal for the laboratory
Severe	Cholestasis (as described earlier) with clinical manifestations including severe pruritus, xanthomata, bone fractures
Excluded	Any of the following Died when younger than age of 5 Liver transplant when younger than age of 5 Biliary diversion when younger than age of 5 History of Kasai procedure Not enough clinical data or currently younger than age 5

Genotyping and Quality Control

There were 234 patients genotyped on the Omni1 (n = 138) and the OmniExpress (n = 96) single-nucleotide polymorphism (SNP) arrays (Illumina, San Diego, CA). Genotype data from both platforms were merged into 1 data set, keeping the 705,132 markers present on both arrays. We followed standard quality control procedures to select samples and SNPs for the association test. SNPs with a minor allele frequency less than 0.05, a missing rate greater than 0.05, or not in Hardy–Weinberg equilibrium ($P_{hwe} < .00001$) were removed. The remaining 579,677 SNP markers were tested for association. Samples with a missing rate greater than 0.05 also were removed. The X chromosome heterozygosity rate also was used as a quality control metric and did not show any inconsistency between reported sex and genotype data.

Individuals of European ancestry accounted for the largest ethnic group in our cohort, and only these samples were used to mitigate biases that may arise from population stratification. European ancestry was inferred by multidimensional scaling with PLINK software.[15] Multidimensional scaling was performed on our samples and a HapMap data set of 4 populations: Utah residents with northern and western Europe ancestry; Han Chinese in Beijing, China; Japanese in Tokyo, Japan; and Yoruba in Ibadan, Nigeria[16] (Supplementary Figure 1). From the first 2 multidimensional scaling components, C1 and C2, patients with $-0.0525 < C1 < -0.04$ and $-0.04 < C2 < -0.03$ were selected as our cohort with European ancestry based on visual inspection.

To identify identical and related individuals, we estimated identity-by-state by genome-wide pairwise comparisons among all patients. We found 11 samples that were

enrolled twice, once in the Children's Hospital of Philadelphia cohort and once in ChiLDReN. There were 3 pairs of monozygotic twins with concordant liver phenotype, therefore only 1 proband from each pair was included in subsequent analysis. The remaining pairs with π greater than 0.15 (indicating relatedness) were accounted for by our knowledge of their relationships, except for 1 pair. We suspect that in this pair the de-identified ChiLDReN proband was the child of the subject who was enrolled in the Children's Hospital of Philadelphia cohort. Because of the small number of enrolled families (n = 19), it was not possible to correlate risk allele with severity among relatives.

SNP Association Analysis

After sample quality control including controlling for population stratification and excluding repeated samples, 97 mild and 64 severe liver disease subjects remained for analysis. Because relatives were included in our data set, we used EMMAX, an implementation of the variance component approach that accounts for sample structure,[17] to test for association. Suggestive evidence for association was considered if SNPs reached the threshold of 1×10^{-5}, which yields approximately 1 false-positive association per GWAS in populations of European ancestry.[18]

For a finer resolution of the candidate regions, we performed imputation with IMPUTE2, using the recommended settings.[19] Reference haplotypes were provided from the 1000 Genomes phase I data set.[20] Following these recommendations, SNPs with imputation quality score INFO less than 0.8 and minor allele frequency less than 0.05 were removed from subsequent analysis. The imputed data set was analyzed by SNPTEST using an additive linear model.[19]

Mouse Lines

Thrombospondin 2 (*Thbs2*)-null mice have been described previously.[21] *Thbs2*–green fluorescent protein (GFP) reporter mice expressing GFP driven by the *Thbs2* promoter were produced by the Gene Expression Nervous System Atlas program using a bacterial artificial chromosome clone spanning 70 kb upstream to 75 kb downstream of the *Thbs2* gene as previously described.[22] Genotyping for all mice was performed by polymerase chain reaction (PCR) analysis using genomic DNA isolated from the tail tip. All procedures involving mice were conducted in accordance with federal guidelines and approved Institutional Animal Care and Use Committee protocols. All animals received humane care according to the criteria outlined in the Guidelines for the Care and Use of Laboratory Animals.

Immunohistochemistry and Immunofluorescence

Standard protocols for immunohistochemistry and immunofluorescence were used on liver tissues from *Thbs2*–GFP reporter, *Thbs2*-null, and control mice. Further technical information including fixation, antibodies used, and antigen retrieval and blocking can be found in Supplementary Table 2. Slides were scanned using the Aperio Scan Scope OS at 20× (Leica Microsystems, Buffalo Grove, IL) for immunohistochemistry and were mounted for viewing with the Olympus BX-51 fluorescent microscope (Olympus, Center Valley, PA) for immunofluorescence.

Laser Capture Microdissection and Complementary DNA Amplification

Two 1-week-old C57BL/6J mouse livers were snap frozen in optimal cutting temperature compound (Sakura Finetak, USA, Inc, Torrance, CA). Each liver was sectioned at 12-μm thickness under RNAse-free conditions and placed on a polyethylene teraphthalate (PET)-membrane framed slide for laser capture microdissection (ASEE Products, Knoxville, TN). Sections were fixed in a brief dehydration with ethanol and xylene using standard protocols. Portal tracts were identified under 10× objective light microscopy using the Nikon Eclipse TE2000-S microscope (Nikon Instruments, Melville, NY) and approximately 12–20 portal tracts were selected and cut using mmiCellTools v2.3 software equipped with a solid-state UV laser (Molecular Machines and Industries, Eching, Germany). The remaining tissue on each section was extracted (liver lobule) to serve as a control and was considered to be enriched for parenchymal transcripts. Samples were collected using PCR sample tubes for laser capture microdissection (ASEE Products). Extraction buffer was applied to samples and they were placed on dry ice until RNA isolation using the PicoPure RNA isolation kit (Life Technologies, Grand Island, NY).

The Ovation Pico WTA System V2 kit was used to produce approximately 10–20 μg of single primer isothermal amplification complementary DNA (cDNA) from approximately 15–25 ng of total RNA (NuGEN Technologies, San Carlos, CA) following their standard protocol. RNA integrity and purity was confirmed before cDNA synthesis using an Agilent 2100 Bioanalyzer (Agilent Technologies, Inc, Wilmington, DE) and a NanoDrop (Wilmington, DE). Amplified products were purified a second time using Qiagen's (Germantown, MD) QIAquick PCR purification kit and cDNA yield and purity was assessed again via both a NanoDrop as well as an Agilent DNA 1000 Bioanalyzer.

Gene Expression Analysis

Droplet digital PCR (ddPCR) was performed on a Bio-Rad QX100 ddPCR system (Hercules, CA) using cDNA harvested from laser capture microdissected tissue kindly provided to us by Dr Matthew Ryan (Division of Gastroenterology, Hepatology, and Nutrition, Children's Hospital of Philadelphia). Droplets containing 60 ng of cDNA from mouse portal tracts were created using TaqMan (Thermo Fisher Scientific, Waltham, MA) mouse *Thbs2* primer and probe set (Mm01279240_m1) with TaqMan primer and probe set for the control gene, *Tbp* (Mm00446971_m1). Standard ddPCR methods were used for experimental conditions and subsequent analysis.[23]

Microvessel, Biliary, and Arterial Counts

Average numbers of microvessels (CD34+) and mature bile ducts (cytokeratin 19 [CK19]+) per portal tract were calculated based on examination of 4 *Thbs2*-null and 4 control 1-week-old and adult livers using immunofluorescence.

Seven to 8 portal tracts were photographed for each sample and portal areas were outlined. Microvessels positively expressing CD34 and mature bile ducts positively expressing CK19 with a visible lumen within the designated portal region were counted and averages were calculated. For arterial counts, immunohistochemistry was performed on paraffin-embedded sections using CK19 and smooth muscle actin antibodies. Four 1-week-old *Thbs2*-null and control livers and 5 adult *Thbs2*-null and control livers were examined. The number of arteries were counted across entire liver sections and quantified by determining the average number of arteries per μm^2. Results of the microvessel and arterial counts are presented as means and SEMs. Data were analyzed using the unpaired *t* test with a 2-tailed *P* value for statistical significance.

Co-immunoprecipitation

The 293A cells plated on 6-well plates were transfected with expression constructs encoding proteins of interest for 48 hours. The immunoprecipitation protocol has been described previously.[24] Plasmids encoding the ectodomains of NOTCH1 and NOTCH2 fused to a C-terminal V5 epitope tag have been described.[25]

Retrovirus Production and Transduction

Phoenix A (amphotropic) cells were plated at a density of 4×10^5 cells/well on a 6-well plate. On the following day, culture media was replaced with fresh media (Dulbecco's modified Eagle medium, high glucose, 10% fetal bovine serum, pen-strep, L-glutamine). Chloroquine dihydrochloride (S764663; Sigma, St. Louis, MO) was added to Phoenix cells 5 minutes before transfection and 2 μg of plasmid DNA was transfected into cells using the Profection kit (E1200; Promega, Madison, WI). The media was changed 10 hours after transfection. Retroviral supernatant was collected the following day and 2 mL was added to GP+E86 cells, plated at 4×10^4 cells/well on a 6-well dish the previous day, after filtration (0.45 μm) and supplemented with protamine sulfate (5 μg/mL). GP+E86 cells were transduced again on the following day. Viral supernatant from GP+E86 cells was collected on the following 2 days and used to transduce C3H10T1/2 cells.

Binding Assays

Recombinant proteins from R&D Systems (Minneapolis, MN) in this study include the following: recombinant human NOTCH2-Fc and NOTCH3-Fc fusions (containing the first 11 epidermal growth factor-like repeats), rat JAG1-Fc, human full-length thrombospondin 2, and control human IgG1 Fc. For protein labeling, 5 μg of protein was incubated with Alexa700-succinimide (10 μg) in phosphate-buffered saline at room temperature for 1 hour. Unincorporated label was removed using a size exclusion column equilibrated in Tris buffer (25-kilodalton cut-off level; Bio-Rad). Labeling of proteins was verified by sodium dodecyl sulfate–polyacrylamide gel electrophoresis under reducing conditions, followed by visualization of label using a LI-COR Odyssey flatbed infrared detector (LI-COR Biosciences, Lincoln, NE). All proteins were predominantly 1 band of the expected molecular weight at an apparent purity of at least 90%. Target proteins were coated on 96-well, flat-bottom enzyme-linked immunosorbent assay plates at 5 μg/mL in Tris-buffered saline (50 mmol/L Tris, 150 mmol/L NaCl) with 2 mmol/L $CaCl_2$ overnight at 4°C and then blocked with 1% bovine serum albumin (BSA) in Tris-buffered saline with 2 mmol/L $CaCl_2$ for 1 hour at room temperature. The wells then were incubated with Alexa700-succinimide–labeled proteins in Tris-buffered saline plus 2 mmol/L $CaCl_2$ and 0.05% Tween 20 at 4°C overnight. In some experiments, unlabeled thrombospondin 2 was added to the binding reaction to assess the effect on binary interactions. Bound, labeled proteins were quantified with a LI-COR Odyssey flatbed infrared detector (LI-COR Biosciences). Ligand binding studies of proteins immobilized on plastic have been described previously.[24] As in the previous study, control studies of the labeled proteins used here showed only trivial amounts of labeling of Fc and BSA control-coated plates.

Generation of Thrombospondin 2 Type I Repeat Deletion Constructs

A retroviral construct missing all 3 type I repeat domains (amino acids 379–549, THBS2-Del3) was generated by PCR amplification of a 1169-base pair fragment encoding amino acids 1–378 (fragment 1) and a 1925-base pair fragment encoding amino acids 550–1172 (fragment 2), followed by cloning into the pCRII-TOPO vector (Invitrogen, Carlsbad, CA). SfoI restriction sites were added to the 3' primer of fragment 1 and the 5' primer of fragment 2 to allow for ligation. Fragments 1 and 2 were released from pCRII-TOPO using BamHI/SfoI and SfoI/XbaI, respectively, and ligated into the pBluescript cloning vector. The full-length THBS2 and THBS2-Del3 fragment were released from pBluescript using EcoRI and cloned into the pRET retroviral vector.

Cell Culture

Stromal cells were harvested from femurs and tibias of *Thbs2*-null and control mice and cultured as previously described.[26] At 80% confluence, cells were trypsinized and plated on 12-well tissue culture plates at a density of 1×10^5 cells per well. Notch signaling was activated by precoating tissue culture plates with 10 μg/mL of antibody against the Fc portion of human IgG (Jackson ImmonoResearch, West Grove, PA) for 1 hour and then incubating with the indicated concentration of recombinant rat JAG1/human Fc IgG chimeric protein (R&D Systems) for 2 hours as previously described.[27] For Notch reporter activity experiments, Fc-JAG1 or TNF-related apoptosis-inducing ligand (control) conditioned media[28] were used to coat plates instead of the recombinant Fc-JAG1 protein.

RNA Extraction and Quantitative Reverse-Transcription PCR

RNA was extracted using the RNeasy RNA extraction kit (Qiagen, Venlo, The Netherlands) according to the

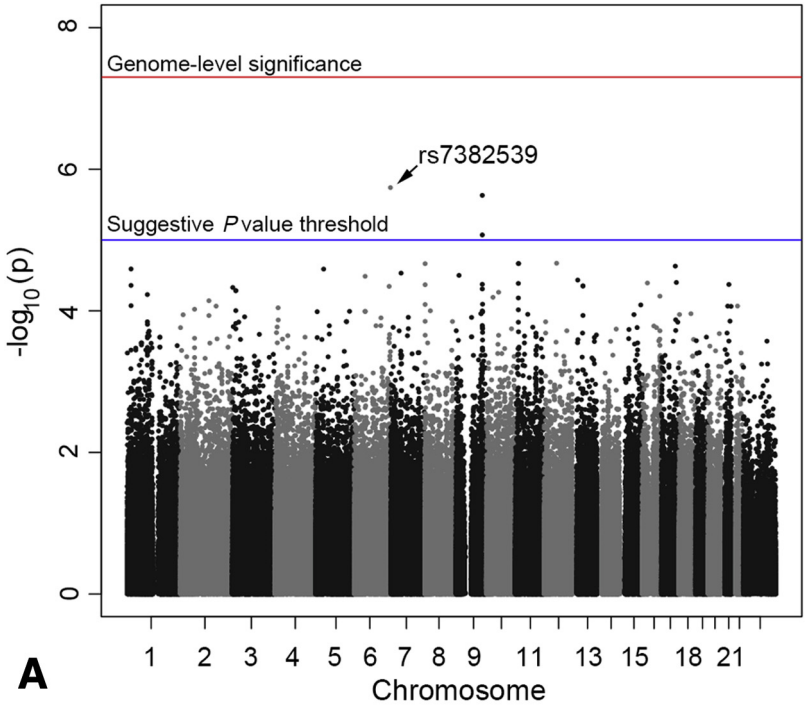

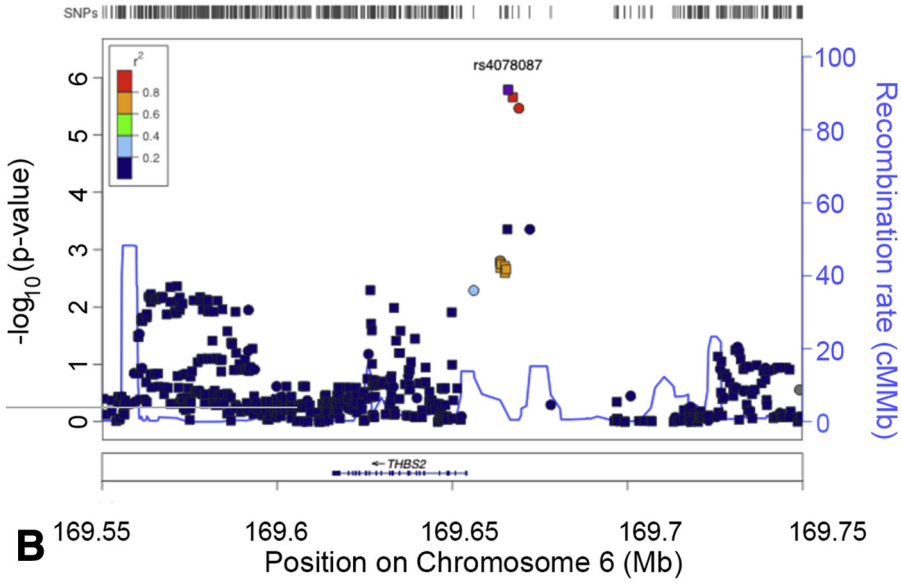

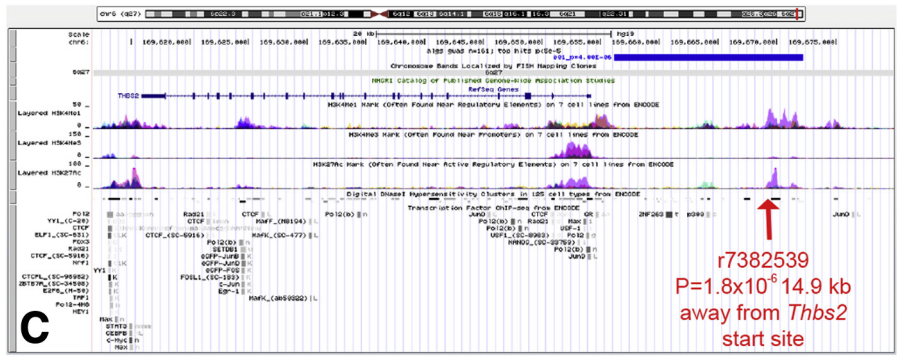

Figure 1. Genotyped and imputed SNPs associated with liver disease severity in ALGS patients. (*A*) Manhattan plot showing all genotyped SNPs. X-axis: genomic coordinates of GWAS tested SNPs from chromosome 1 to X. Y-axis: significance level for each SNP on a -$\log_{10}$ scale. Genome-level significance, $P = 5 \times 10^{-8}$; suggestive P value threshold, $P = 1 \times 10^{-5}$. (*B*) Regional association plot of 6q27. P values (left Y-axis) obtained from an additive linear test on the genotyped (*circle*, rs7382539) and imputed (*square*, rs4078087 and rs7451470) markers in the *THBS2* genomic region (X-axis). The recombination rate (right Y-axis) is calculated from the 1000 Genomes Phase I data set of subjects with European ancestry. The top 3 markers are in strong linkage disequilibrium with each other ($r^2 = 1$). (*C*) The top SNP signal is shown with the proximal *THBS2* gene. The *red arrow* indicates the site of the top signal from the SNP association study. This region also is marked by acetylated histone H3 lysine 27 (H3K27Ac) and monomethylated histone H3 lysine 4 (H3K4Me1) peaks. The *solid blue bar* depicts the region of linkage disequilibrium including SNP markers with $r^2 > 0.2$ with rs7382539.

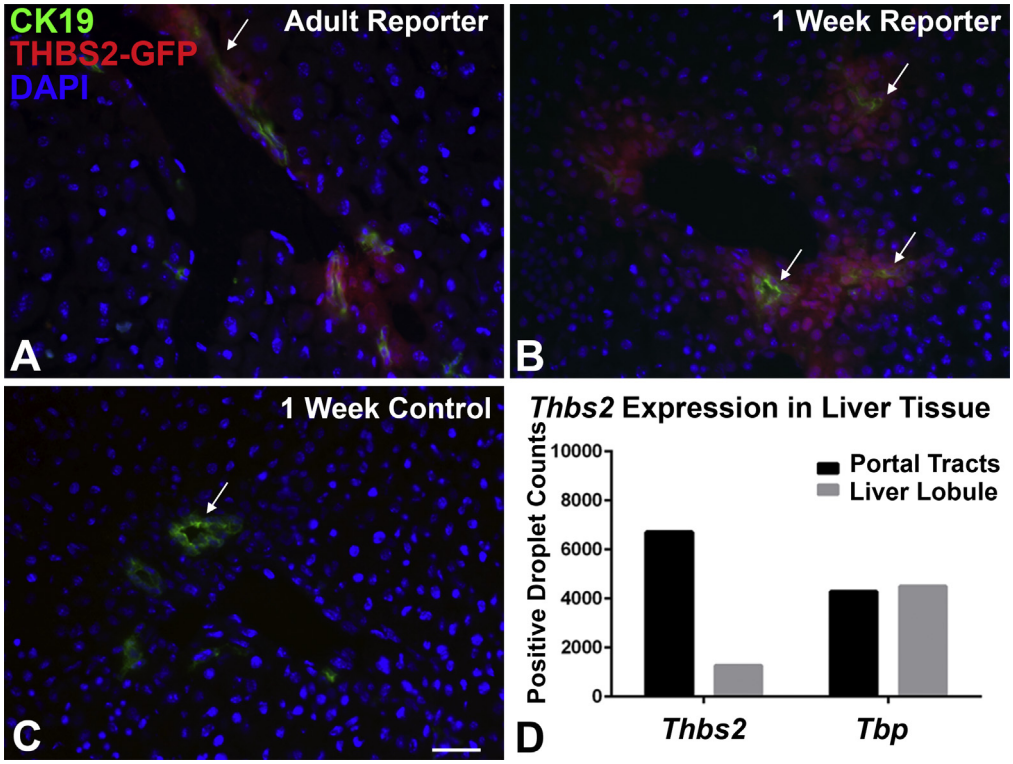

Figure 2. Expression of thrombospondin 2 in mouse portal tracts and bile ducts. (*A*) The adult *Thbs2*–GFP reporter (red) mouse liver shows co-localization of thrombospondin 2 with the mature biliary marker CK19, (*B*) with broader expression seen at 1 week of age. (*C*) A 1-week-old littermate control lacking the GFP reporter shows CK19 expression only. (*D*) ddPCR shows that *Thbs2* expression is increased by more than 5-fold in laser-captured portal tracts when compared with the remaining liver lobule (N = 2). No change in expression between the 2 tissue types is seen with the control gene, *Tbp*. (*A–C*) Antibodies against GFP were used. *Arrows* indicate co-localization of (*A* and *B*) thrombospondin 2 and CK19 and (*C*) CK19 expression alone. Images were obtained using the Aperio Scan Scope OS (Leica Microsystems) at 20×. *Scale bar*: 25 μm. DAPI, 4′,6-diamidino-2-phenylindole.

manufacturer's instructions and 1 μg of total RNA was reverse-transcribed. Quantitative real-time PCR reactions using SybrGreen I were performed on an ABI 7500 Fast Real-Time PCR System (Life Technologies, Carlsbad, CA). Relative changes in gene expression were determined by the $2^{\Delta\Delta CT}$ method using β-actin as an endogenous control.

Transient Transfection and CSL-Luciferase Assay

C3H10T1/2 cells were plated on 12-well plates coated with either Fc-Trail or Fc-JAG1 recombinant protein. After 36 hours, cells were co-transfected with 0.5 μg of CSL-luciferase, a synthetic DNA construct in which 4 tandem repeats of CBF-1, Suppressor of Hairless, Lag-1 binding elements drive expression of firefly luciferase, and 100 ng of pRL-TK, a constitutively active TK promoter driving expression of renilla luciferase activity, using Lipofectamine and Plus reagent (Invitrogen). Cells were harvested 48 hours after transfection and firefly and renilla luciferase activities were measured using the Dual Luciferase assay kit (Promega).

Immunoblotting

Protein was extracted from cultured human fibroblast samples using RIPA buffer (Sigma-Aldrich, St. Louis, MO) supplemented with proteinase inhibitors (Thermo Fisher Scientific). All Western blots were run using NuPAGE Tris-acetate pre-cast gels (Thermo Fisher Scientific). Membranes were blocked with 5% milk and 2% BSA and incubated for either 1 (β-actin, 1:5000) or 2 (thrombospondin 2, 1:50) nights with primary antibody. Membranes were incubated in horseradish-peroxidase–conjugated secondary antibody for 1 hour at room temperature and subsequently were developed using Pierce ECL Western Blotting Substrate (Thermo Fisher Scientific). Antibodies used included thrombospondin 2 (BD Biosciences, San Jose, CA) and β-actin (Millipore, Billerica, MA). Thrombospondin 2 expression was quantified and normalized to β-actin using ImageJ software (National Institutes of Health, Bethesda, MD).

Results

SNP Association Analysis

We performed a GWAS to identify common genetic variants influencing the severity of the hepatic phenotype in ALGS. Although we did not observe any inflation in the Q-Q plot of the observed against the expected *P* values ($\lambda = 1.005$), indicating the quality control and analysis methods correctly accounted for any potential population stratification (Supplementary Figure 2), none of the markers passed

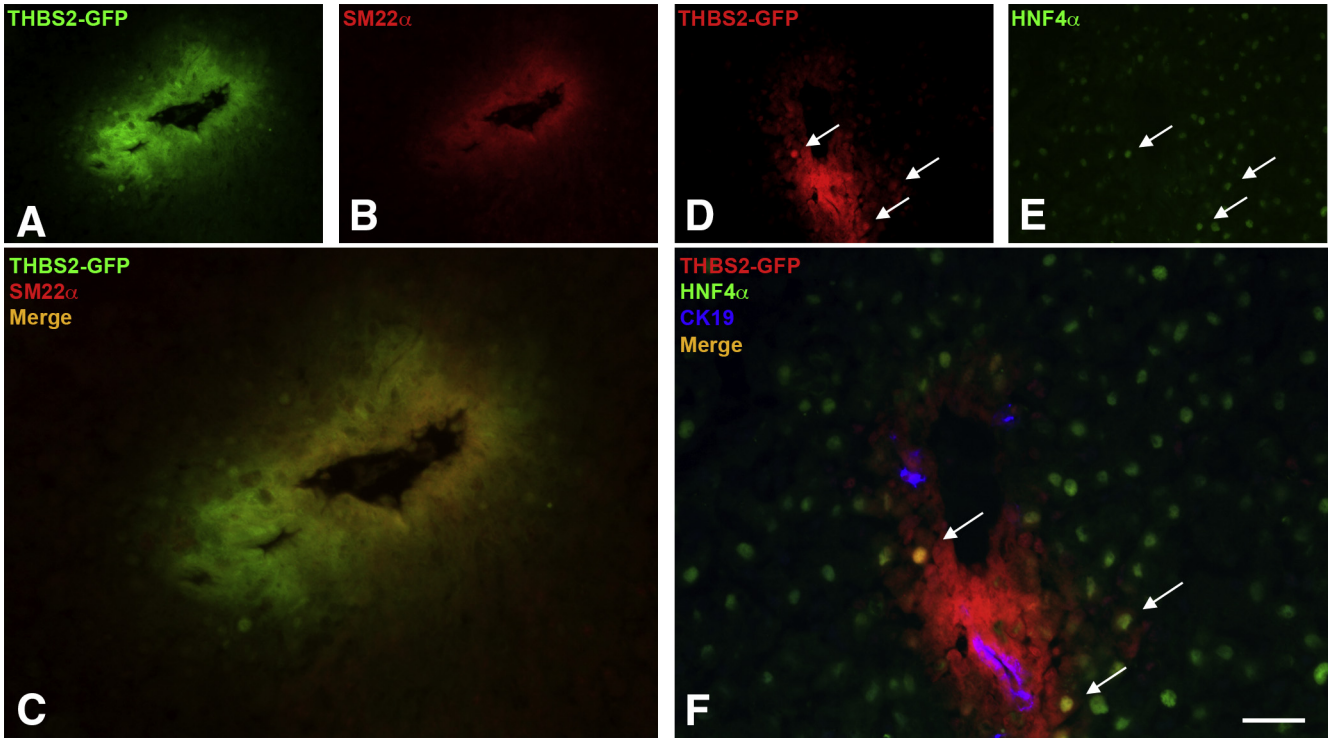

Figure 3. Thrombospondin 2 is expressed in periportal mesenchyme and hepatocytes in mouse liver at 1 week of age. (*A–C*) Thrombospondin 2 (GFP-green) co-localizes with the mesenchymal marker smooth muscle 22α (SM22α). (*D–F*) Thrombospondin 2 (GFP-red) rarely is expressed in periportal hepatocytes (hepatocyte nuclear factor 4 α [HNF4α], *arrows*). Bile ducts are labeled with CK19. Antibodies against GFP were used. *Arrows* indicate colocalization of GFP and HNF4α. Images were obtained using the Aperio Scan Scope OS (Leica Microsystems) at 20×. *Scale bar*: 25 μm.

the threshold for genome-wide significance ($P < 5 \times 10^{-8}$). However, 1 marker in 6q27 (rs7382539; $P = 1.8 \times 10^{-6}$) and 2 markers in 9q33.2 (rs944961; $P = 2.3 \times 10^{-6}$; and rs2900162; $P = 8.5 \times 10^{-6}$) reached the suggestive *P* value threshold ($P < 1 \times 10^{-5}$) (Figure 1*A*).

The most significant marker, rs7382539, was located at 6q27, 14-kb upstream of *THBS2*. This marker is in moderate linkage disequilibrium ($r^2 > 0.2$) with SNPs up to approximately 2 kb upstream of *THBS2* in the 1000 Genomes European superpopulation (Figure 1*C*). After imputation, 2 additional SNPs, rs4078087 and rs7451470, showed the same magnitude of significance as rs7382539 (Figure 1*B*). These 3 SNPs are correlated strongly with each other ($r^2 = 1$). Upon inspection of the Encyclopedia of DNA Elements histone modification peaks in this marker region,[29] we observed histone marks that may be indicative of enhancer activity for both acetylated histone H3 lysine 27 and monomethylated histone H3 lysine 4 (Figure 1*C*).[30]

The second and third ranking markers were located on 9q33.2, almost 500 kb away from the nearest flanking genes, deleted in bladder cancer protein 1 (*DBC1*) and CDK5 regulatory subunit-associated protein 2 (*CDK5RAP2*). The linkage disequilibrium block around these markers does not include these genes. The region tagged by these markers did not have any histone modification peaks and was not in any DNase I hypersensitivity clusters.[29] Imputed SNPs did not

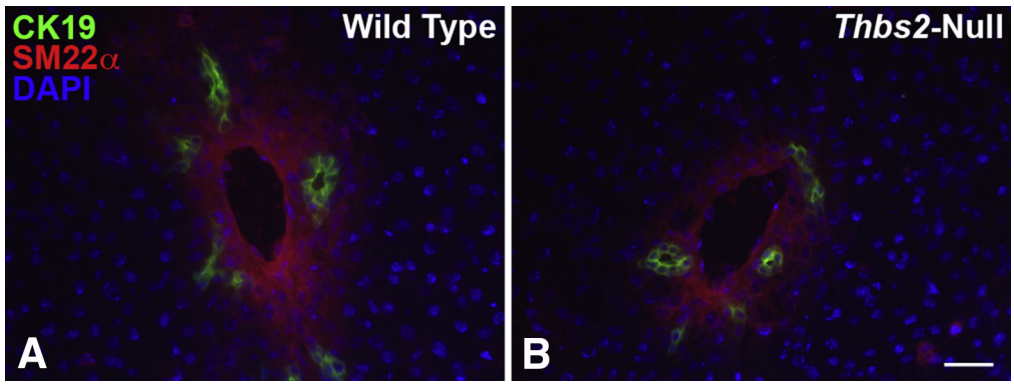

Figure 4. Normal bile ducts in *Thbs2*-null mouse liver. Immunofluorescence staining for bile duct marker CK19 and mesenchymal marker smooth muscle 22α (SM22α) shows normal bile duct structures in the portal tracts of (*A*) control and (*B*) *Thbs2*-null mouse livers at 1 week of age. *Scale bar*: 25 μm. DAPI, 4′,6-diamidino-2-phenylindole.

Table 2. Average Number of Microvessels and Bile Ducts per Portal Tract in 1-Week-Old and Adult Control and Thbs2-Null Livers

Age	Genotype	Average microvessels, n	*P* value	Average bile ducts, n	*P* value
1 week	*Thbs2*-null	7.6 ± 0.5	.680	1.9 ± 0.2	1.000
	Control	8.0 ± 0.7		1.9 ± 0.2	
Adult	*Thbs2*-null	12.1 ± 0.7	.001	2.3 ± 0.2	.460
	Control	9.1 ± 0.5		2.1 ± 0.2	

reach greater significance than the genotyped markers and these were not analyzed further.

Thrombospondin 2 Is Expressed in Biliary Epithelium and Portal Regions of the Mouse Liver

Although our GWAS did not identify any markers that reached genome-wide significance, we were intrigued to investigate the functional role of thrombospondin 2 given the known interaction of thrombospondin 2 with Notch proteins[24] and the fundamental importance of Notch signaling in ALGS. As a first step toward interpreting the potential significance of the signal near *THBS2*, we analyzed the expression pattern of thrombospondin 2 in the liver. This was performed using a reporter mouse line expressing GFP driven by the *Thbs2* promoter (*Thbs2*-GFP). Examination of adult mouse livers showed co-localization of biliary marker CK19 with GFP, indicating that thrombospondin 2 is expressed in bile ducts (Figure 2*A*, arrow). Thrombospondin 2 expression in the adult mouse liver was confined to the periportal regions with no parenchymal expression. One-week-old *Thbs2*–GFP reporter livers also were examined. Again, CK19 co-localized with GFP, indicating thrombospondin 2 expression in biliary epithelium (Figure 2*B*, arrows). Of notable difference at the earlier time point is the broader expression of thrombospondin 2 surrounding the portal tracts, appearing to include mesenchymal cells and periportal hepatocytes (Figure 3). Staining in control littermates was negative for GFP, as expected (Figure 2*C*).

To confirm these results, we examined expression levels of *Thbs2* messenger RNA transcripts in laser-captured mouse portal tracts vs the remainder of the liver lobule using ddPCR. cDNA amplified from control livers at 2 weeks of age showed greater than a 5-fold increase in *Thbs2* expression in the portal tracts vs the liver lobule (Figure 2*D*). Thus, examination of *Thbs2* messenger RNA expression and thrombospondin 2 protein localization using a GFP reporter mouse confirm enrichment of thrombospondin 2 in portal regions, with specific expression in biliary epithelium, mesenchyme, and, rarely, in hepatocytes.

Thbs2-*Null Mice Have Increased Microvessels in Portal Regions*

We examined *Thbs2*-null mouse livers at 12 weeks of age and compared them with littermate controls. Liver histology was unremarkable by H&E staining, and Sirius red staining did not show fibrosis in the mutant livers (data not shown). Immunofluorescence staining for CK19 showed normal numbers and structure of bile ducts in the *Thbs2*-null mice (Figure 4). *Thbs2*-null animals show increased vascularity in different tissues including the eye,[31,32] brain,[33] skin,[21] heart,[34] and bone.[35] We examined *Thbs2*-null and littermate control livers at 1 and 12 weeks of age using CK19 and CD34 antibodies to estimate the average number of bile ducts and microvessels per portal tract (Table 2). The average number of bile ducts was approximately 2 per portal tract in the *Thbs2*-null and control livers at both time points. However, we identified a higher average number of microvessels per portal tract in adult *Thbs2*-null livers over littermate controls, expanding upon the already reported phenotype of increased vascularity seen in other *Thbs2*-null tissues. To refine our assessment, we calculated the size of each portal tract and verified that areas examined among mutant and control portal tracts were similar (data not shown). This difference in the number of microvessels per portal tract was not seen in the younger cohort.

In addition, we stained *Thbs2*-null and littermate control livers with smooth muscle actin to identify mature arteries in portal tracts at 1 and 12 weeks of age. Interestingly, we identified more arteries in the 1-week-old *Thbs2*-null livers compared with controls, with approximately 10.5 arteries in the nulls and 4.5 in controls (Table 3). Taking into account the area of each liver section, the increase in the number of arteries per μm^2 was statistically significant ($P = .01$). Curiously, the opposite was found in the adult liver, in which *Thbs2*-null livers had, on average, 23.8 arteries, whereas controls showed 33.2 arteries ($P = .05$). After normalization by area, the numbers followed the same trend, but they were no longer significant ($P = .14$).

Table 3. Average Number of Arteries in 1-Week-Old and Adult Control and Thbs2-Null Liver Sections

Age	Genotype	Average arteries, n	*P* value	Average arteries, n, $\mu mol/L^2$	*P* value
1 week	*Thbs2*-null	10.5 ± 1.4	.010	3.7×10^{-7}	.010
	Control	4.5 ± 0.9		1.7×10^{-7}	
Adult	*Thbs2*-null	23.8 ± 2.5	.050	2.7×10^{-7}	.140
	Control	33.2 ± 3.4		3.6×10^{-7}	

Thrombospondin 2 Affects JAG1–NOTCH2 Interactions In Vitro

Given the crucial role of JAG1–NOTCH2 interactions in bile duct development, we performed *in vitro* binding assays using purified proteins to determine the effect of thrombospondin 2 on JAG1–NOTCH2 binding. We found that thrombospondin 2 can be isolated from protein complexes containing either NOTCH1 or NOTCH2 ectodomains (Figure 5*A*). We further found that when the JAG1 ectodomain is labeled and incubated on NOTCH2 ectodomain-coated wells, addition of thrombospondin 2, but not BSA, is able to strongly inhibit JAG1–NOTCH2 binding (Figure 5*B*). In addition, increasing concentrations of thrombospondin 2 inhibited formation of complexes that included JAG1 and NOTCH2 (Figure 5*C*). Interestingly, thrombospondin 2 enhances formation of complexes that include JAG1 and NOTCH3 binding in this same assay (Figure 5*C*). These results indicate that thrombospondin 2 is able to interact directly with Notch proteins and interfere with JAG1–NOTCH2 complex formation.

To determine the effects of thrombospondin 2 on Notch pathway signaling, we assayed downstream gene expression using stromal cells harvested from *Thbs2*-null mice and exposed to JAG1 protein. We found that Notch pathway target genes were markedly upregulated in the *Thbs2*-null cells in a dose-dependent manner after exposure to JAG1 (Figure 6*A*). The most profound difference in both expression and JAG1 dose response between *Thbs2*-null and control stromal cells occurred with *Hey-L* expression (Figure 6*A*). Conversely, overexpression of thrombospondin 2 *in vitro* resulted in reduced Notch pathway activation with at least 50% reduced expression of *Hey1* compared with controls (Figure 6*B*). Overexpression of a modified thrombospondin 2 construct lacking the type I repeat domain (THBS2-Del3) did not reduce *Hey1* expression as compared with control after exposure to JAG1 (Figure 7). A Notch luciferase reporter assay also showed a decrease in luciferase activity after overexpression of the full-length thrombospondin 2 protein, confirming that thrombospondin 2 inhibits canonical Notch signaling in this model (Figure 6*C*).

We attempted to investigate whether the risk allele identified in the GWAS affected thrombospondin 2 RNA or protein expression. Thrombospondin 2 is not expressed in lymphoblastoid cell lines, so we studied fibroblast cell lines derived from ALGS and control individuals of different genotypes. In control fibroblast cell lines, we identified a trend toward increased thrombospondin 2 protein expression in individuals heterozygous (AG; mean fold difference over control, 5.72; n = 5) and homozygous (AA; mean fold difference over control, 7.65; n = 2) for the risk allele compared with those homozygous for the nonrisk allele (GG; mean fold difference over control, 2.10; n = 3), which would support our hypothesis (Figure 8*A*). In the ALGS fibroblast samples, thrombospondin 2 protein expression was extremely variable and there was no clear evidence of correlation between genotype (AA; n = 2) and expression level (Figure 8*B*). Thrombospondin 2 RNA expression also showed no correlation between genotype and expression level (data not shown). We are cautious about interpreting these findings both owing to the very low sample size we had for both populations and the tissue type examined. Ideally, we would like to study this type of correlation in liver tissue, but it was not available to us at this time. Further studies will be required to determine whether the GWAS-identified SNP directly or indirectly regulates THBS2 expression, and if this effect is tissue specific.

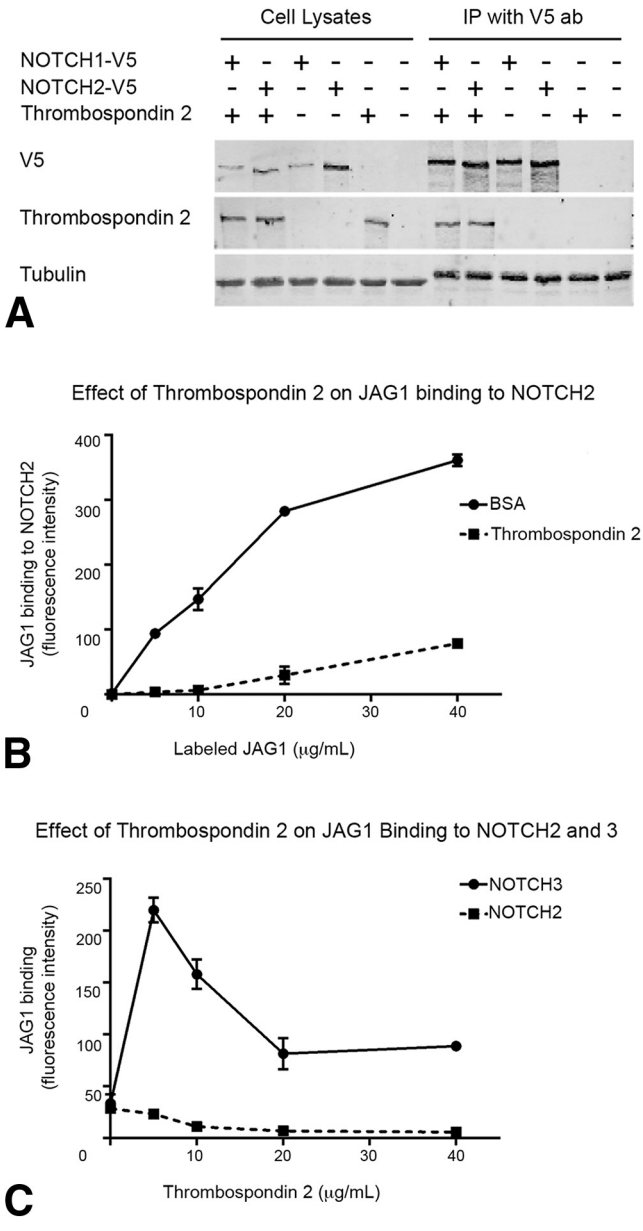

Figure 5. Thrombospondin 2 interacts with Notch *in vitro*. (*A*) Immunoprecipitation of NOTCH1–V5, NOTCH2–V5, and thrombospondin 2 with indicated antibodies. (*B*) Solid phase binding assay to test the ability of thrombospondin 2 to inhibit the interaction of the JAG1 ectodomain with NOTCH2. (*C*) Competitive binding assay incubating increasing concentrations of unlabeled thrombospondin 2 in NOTCH2 or NOTCH3 ectodomain-coated wells with a fixed concentration of JAG1 ectodomain.

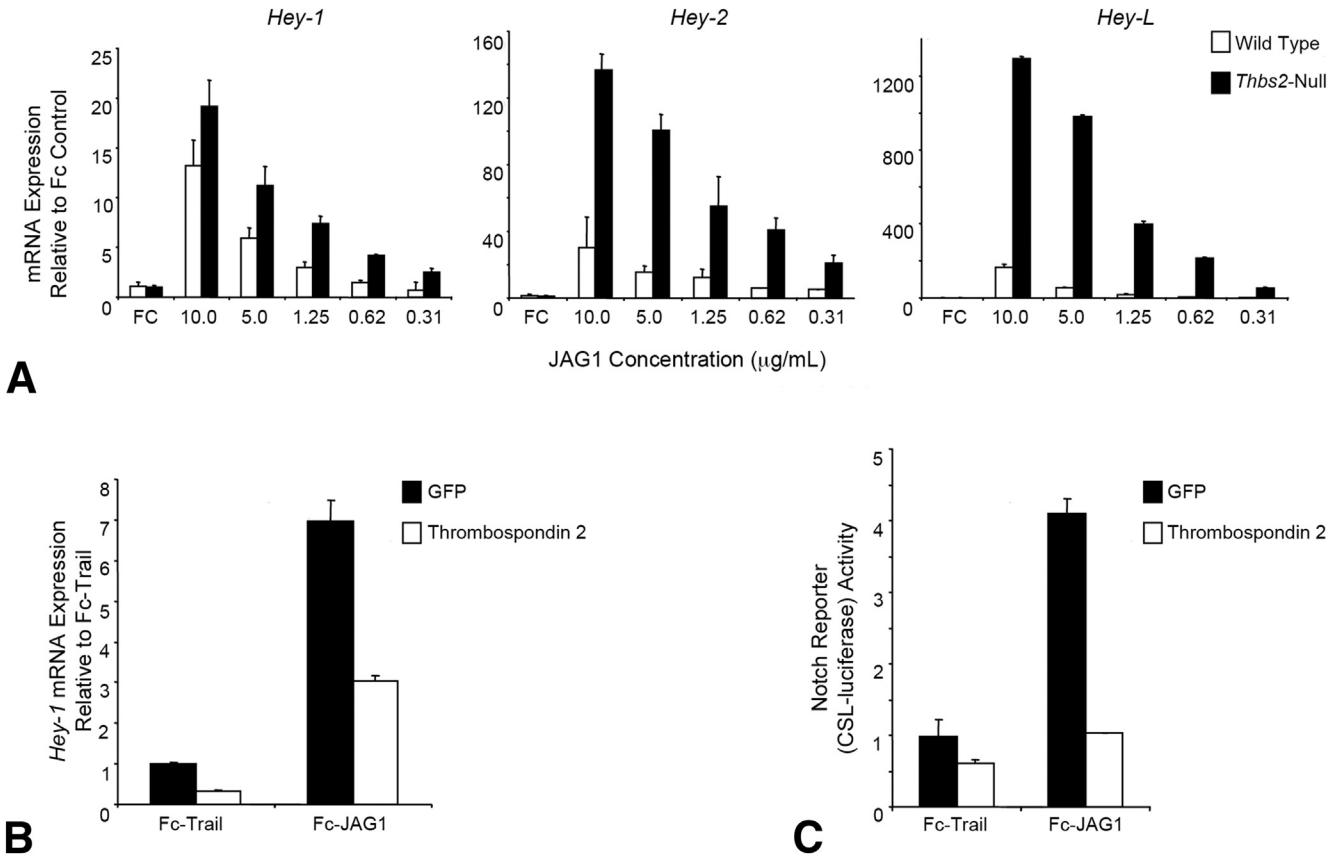

Figure 6. *Thbs2* expression alters Notch target gene expression. (*A*) Gene expression analysis by quantitative PCR of *Thbs2*-null stromal cells shows up regulation of 3 Notch target genes in response to varying doses of JAG1 recombinant protein. (*B*) Gene expression analysis by quantitative PCR shows reduced *Hey1* messenger RNA (mRNA) expression when C3H10T1/2 cells are transfected with a retrovirus expressing thrombospondin 2 relative to GFP. (*C*) A luciferase assay measuring Notch activity shows that luciferase activity normalized to pRL-TK was decreased in thrombospondin 2–overexpressing cells relative to GFP-overexpressing cells.

Discussion

Our study has identified *THBS2* as a compelling candidate modifier gene of liver disease severity in ALGS. Thrombospondin 2 is a matricellular protein that previously was shown to potentiate JAG1–NOTCH3 interactions—a function that is specific to thrombospondin 2 and not other thrombospondin family members.[24] Although thrombospondin 2 has been studied in other tissues and found to be associated with anti-angiogenic effects during wound healing,[36] its role in the liver has not been studied to date. Given the importance of both the *JAG1* gene and Notch signaling in the etiology of ALGS, we pursued additional functional studies after identifying this gene through our GWAS. We further show that thrombospondin 2 interacts with NOTCH1 and NOTCH2, and that increased concentration of thrombospondin 2 results in reduced binding of the JAG1–NOTCH2 ligand-receptor pair. We also show that thrombospondin 2 is expressed specifically in the biliary epithelium and portal tracts of mouse liver (Figure 2). Together these data are highly suggestive of a role for thrombospondin 2 in the liver phenotype of ALGS.

Through the GWAS, we identified a SNP, rs7382539, located 14 kb upstream of *THBS2* on 6q27, that is associated with liver disease severity in ALGS patients with a JAG1 mutation. Although rs7382539 did not pass the cut-off for genome-wide significance, it did reach a suggestive level of significance for European populations. We identified 2 additional SNPs, rs4078087 and rs7451470, in strong linkage disequilibrium with each other and with rs7382539 ($r^2 = 1$) and highly associated with liver disease severity through imputation (Figure 1). These 3 SNPs are located in regions with histone marks that are indicative of enhancer activity, including acetylated histone H3 lysine 27 and monomethylated histone H3 lysine 4.[30] This suggests that although the causal marker may not be in the coding sequence of *THBS2*, it still potentially can play a role in regulating this gene.

By using a reporter mouse, we identified a pattern of expression for thrombospondin 2 in the portal tracts and biliary epithelium of the adult liver (Figure 2) and showed that this pattern extends into stromal cells and is seen rarely in periportal hepatocytes in young mice (1 week old) (Figure 3). Studies aiming to identify expression patterns of thrombospondin 2 during murine embryogenesis found high levels of expression in the heart, vessels, and mesenchyme.[37] In addition, a role for thrombospondin 2 in

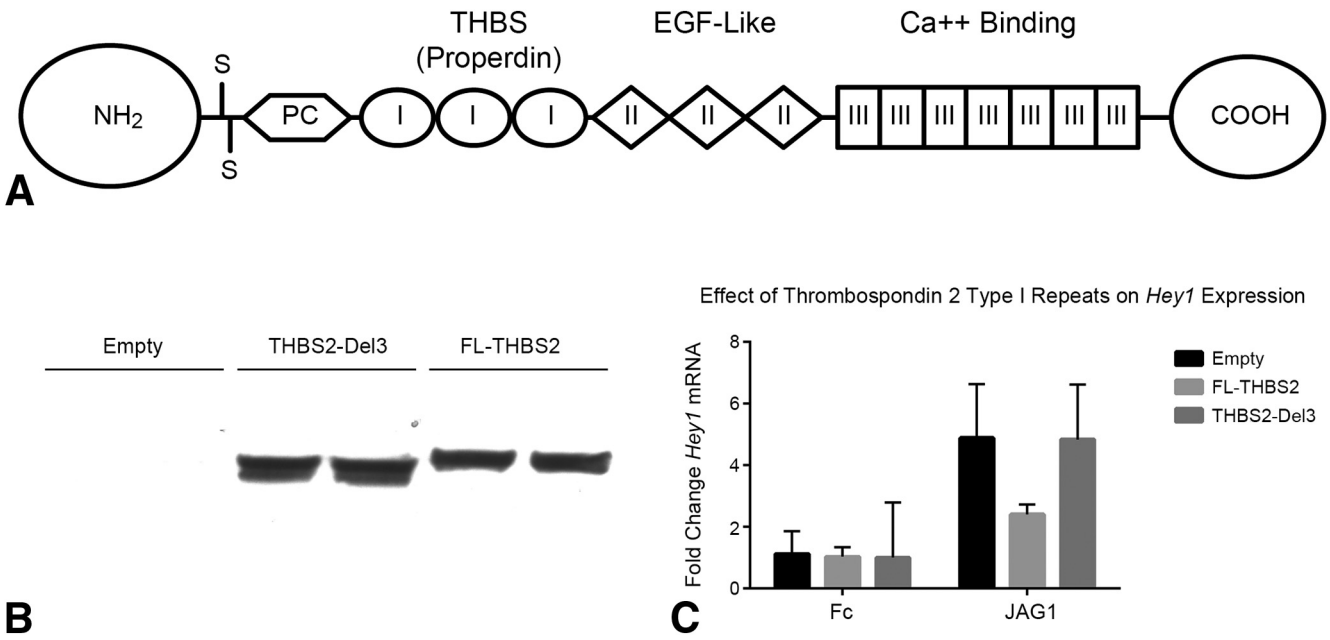

Figure 7. Type I repeats of *THBS2* are required to inhibit *Hey1* expression. (*A*) Schematic of the *THBS2* gene showing type I repeat domains. (*B*) Western blot showing thrombospondin 2 secretion into media by stably transduced C3H10T1/2 cells of empty vector, thrombospondin 2 in which all 3 type I repeat domains have been deleted (THBS2-Del3), and full-length thrombospondin 2 protein (FL-THBS2). (*C*) Empty vector–, FL-THBS2–, or THBS2-Del3–transduced cells were plated on either Fc-control– (Fc) or recombinant JAG1-coated plates and *Hey-1* mRNA expression was analyzed 4 days later. EGF, epidermal growth factor; PC, procollagen.

angiogenesis has been well described for multiple tissue types.[21, 31–35] A recent report identified a thinning of periportal vascular smooth muscle cells in mice haploinsufficient for *Jag1*, suggesting that an angiogenic effect associated with Notch signaling also is seen in the liver.[38] We investigated a role for thrombospondin 2 in liver vasculature and found that adult mice lacking thrombospondin 2 had increased numbers of microvessels per portal tract whereas 1-week-old mice, but not adult mice, showed an increase in the number of arteries per portal tract (Tables 2 and 3). This finding is in keeping with the results of Krady et al,[39] who found an increase in baseline arteriogenesis in *Thbs2*-null animals in an induced-ischemia model of the hindlimb. Our finding within the 1-week-old livers raises the possibility that the rate at which arteries develop may be increased in the *Thbs2*-null livers, but that once maturity is reached, the number of arteries either normalizes or is reduced slightly. Our results both substantiate our expression data and suggest that thrombospondin 2 may have combined roles in biliary development and liver vasculature. In addition, they suggest that it may be interesting to investigate thrombospondin 2 as a modifier of the heart and vascular phenotypes in ALGS. Indeed, recent studies have found an association of *THBS2* with a variety of heart conditions, including coronary artery disease,[40,41] thoracic aortic dissection,[42] and heart failure with preserved ejection fraction.[43]

Biologically, *THBS2* represents an intriguing putative modifier of ALGS liver disease severity because it previously has been shown in binding assays that thrombospondin 2 is capable of physically binding to NOTCH3 and JAG1.[24] Here, we extended these observations and show that thrombospondin 2 also interacts with NOTCH2 (Figure 5) and inhibits the expression of downstream Notch target genes in the presence of JAG1 (Figure 6). Moreover, we determined that a specific *THBS2* regulatory domain, the type I repeat, is required for this function (Figure 7). Type I repeats are known to be required for binding to CD36, a glycoprotein expressed on platelets, and for the antiangiogenic function of thrombospondin 2.[44] Given the increased numbers of microvessels and arteries in *Thbs2*-null adult and 1-week-old mice, respectively, these data suggest that thrombospondin 2 may function via Notch signaling in the liver vasculature such that enhanced thrombospondin 2 levels could decrease Notch signaling and impair angiogenesis during liver development, thereby modifying the liver phenotype in ALGS. The precise molecular mechanism of how thrombospondin 2 blocks NOTCH2 function remains to be determined. Further studies will be needed to distinguish between competitive inhibition of JAG1–NOTCH2 inhibition by thrombospondin 2 vs the allosteric effect of thrombospondin 2 on one of the binding partners.

We acknowledge that our study had several limitations. First, because of the rarity of the syndrome, our patient cohort was small and the marker identified in the GWAS at 6q27 did not reach genome-wide statistical significance. However, given the known interaction of thrombospondin 2 with JAG1/NOTCH3, we were interested in further pursuing

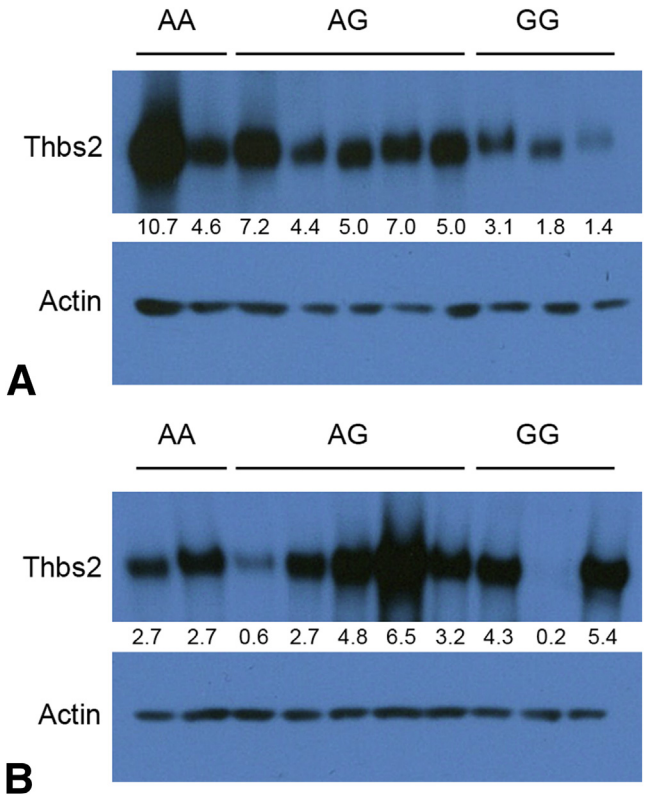

Figure 8. Thrombospondin 2 expression levels in human fibroblasts. (*A*) Thrombospondin 2 expression is higher in control fibroblasts that are heterozygous or homozygous for the risk allele (AG or AA) compared with those homozygous for the nonrisk allele (GG). (*B*) There is no correlation between thrombospondin 2 expression and genotype in disease fibroblasts. Densitometry measurements are shown below each Thbs2 blot and were quantified in ImageJ by normalizing to actin.

functional studies in the liver.[24] Second, we were unable to show a significant correlation between SNP genotype and *THBS2* expression level. It is possible that the GWAS-identified SNP, located upstream of the *THBS2* locus in a region with histone acetylation signatures, functions to regulate *THBS2* expression in a tissue-specific manner. Investigation of this possibility is outside the scope of the current study, but might include chromosome conformation capture, more detailed analysis of patient liver samples, and studies in animal models. Despite these limitations, we believe that the expression data and functional studies provide compelling evidence that thrombospondin 2 could modulate JAG1–NOTCH2 interactions, thereby modifying liver disease severity in ALGS.

Ultimately, these data provide genetic, expression, and functional evidence to support a role for *THBS2* as a modifier of liver disease severity in ALGS. These findings could have significant clinical applications when the current treatment course of liver disease is unpredictable,[9] and the identification of a genetic modifier may help in identifying patient populations that will require liver transplantation at an earlier age.

References

1. Alagille D, Odievre M, Gautier M, et al. Hepatic ductular hypoplasia associated with characteristic facies, vertebral malformations, retarded physical, mental, and sexual development, and cardiac murmur. J Pediatr 1975; 86:63–71.
2. Dhorne-Pollet S, Deleuze JF, Hadchouel M, et al. Segregation analysis of Alagille syndrome. J Med Genet 1994;31:453–457.
3. Elmslie FV, Vivian AJ, Gardiner H, et al. Alagille syndrome: family studies. J Med Genet 1995;32:264–268.
4. Shulman SA, Hyams JS, Gunta R, et al. Arteriohepatic dysplasia (Alagille syndrome): extreme variability among affected family members. Am J Med Genet 1984; 19:325–332.
5. Emerick KM, Rand EB, Goldmuntz E, et al. Features of Alagille syndrome in 92 patients: frequency and relation to prognosis. Hepatology 1999;29:822–829.
6. Hoffenberg EJ, Narkewicz MR, Sondheimer JM, et al. Outcome of syndromic paucity of interlobular bile ducts (Alagille syndrome) with onset of cholestasis in infancy. J Pediatr 1995;127:220–224.
7. Lykavieris P, Hadchouel M, Chardot C, et al. Outcome of liver disease in children with Alagille syndrome: a study of 163 patients. Gut 2001;49:431–435.
8. Quiros-Tejeira RE, Ament ME, Heyman MB, et al. Variable morbidity in Alagille syndrome: a review of 43 cases. J Pediatr Gastroenterol Nutr 1999;29:431–437.
9. Kamath BM, Munoz PS, Bab N, et al. A longitudinal study to identify laboratory predictors of liver disease outcome in Alagille syndrome. J Pediatr Gastroenterol Nutr 2010; 50:526–530.
10. Mouzaki M, Bass LM, Sokol RJ, et al. Early life predictive markers of liver disease outcome in an international, multi-center cohort of children with Alagille syndrome. Liver Int 2016;36:755–760.
11. Crosnier C, Driancourt C, Raynaud N, et al. Mutations in JAGGED1 gene are predominantly sporadic in Alagille syndrome. Gastroenterology 1999;116:1141–1148.
12. Krantz ID, Colliton RP, Genin A, et al. Spectrum and frequency of jagged1 (JAG1) mutations in Alagille syndrome patients and their families. Am J Hum Genet 1998; 62:1361–1369.
13. McElhinney DB, Krantz ID, Bason L, et al. Analysis of cardiovascular phenotype and genotype-phenotype correlation in individuals with a JAG1 mutation and/or Alagille syndrome. Circulation 2002;106: 2567–2574.
14. Spinner NB, Colliton RP, Crosnier C, et al. Jagged1 mutations in Alagille syndrome. Hum Mutat 2001; 17:18–33.
15. Purcell S, Neale B, Todd-Brown K, et al. PLINK: a tool set for whole-genome association and population-based linkage analyses. Am J Hum Genet 2007;81:559–575.
16. The International HapMap Project. Nature 2003; 426:789–796.
17. Kang HM, Sul JH, Service SK, et al. Variance component model to account for sample structure in genome-wide association studies. Nat Genet 2010;42:348–354.

18. Duggal P, Gillanders EM, Holmes TN, et al. Establishing an adjusted p-value threshold to control the family-wide type 1 error in genome wide association studies. BMC Genomics 2008;9:516.
19. Marchini J, Howie B. Genotype imputation for genome-wide association studies. Nat Rev Genet 2010;11:499–511.
20. 1000 Genomes Project Consortium, Abecasis GR, Auton A, et al. An integrated map of genetic variation from 1,092 human genomes. Nature 2012;491:56–65.
21. Kyriakides TR, Zhu YH, Smith LT, et al. Mice that lack thrombospondin 2 display connective tissue abnormalities that are associated with disordered collagen fibrillogenesis, an increased vascular density, and a bleeding diathesis. J Cell Biol 1998;140:419–430.
22. Palenski TL, Gurel Z, Sorenson CM, et al. Cyp1B1 expression promotes angiogenesis by suppressing NF-kappaB activity. Am J Physiol Cell Physiol 2013; 305:C1170–C1184.
23. Tsai EA, Grochowski CM, Falsey AM, et al. Heterozygous deletion of FOXA2 segregates with disease in a family with heterotaxy, panhypopituitarism, and biliary atresia. Hum Mutat 2015;36:631–637.
24. Meng H, Zhang X, Hankenson KD, et al. Thrombospondin 2 potentiates notch3/jagged1 signaling. J Biol Chem 2009;284:7866–7874.
25. Meng H, Zhang X, Yu G, et al. Biochemical characterization and cellular effects of CADASIL mutants of NOTCH3. PLoS One 2012;7:e44964.
26. Hankenson KD, Bornstein P. The secreted protein thrombospondin 2 is an autocrine inhibitor of marrow stromal cell proliferation. J Bone Miner Res 2002;17:415–425.
27. Zhu F, Sweetwyne MT, Hankenson KD. PKCdelta is required for Jagged-1 induction of human mesenchymal stem cell osteogenic differentiation. Stem Cells 2013; 31:1181–1192.
28. Buas MF, Kabak S, Kadesch T. Inhibition of myogenesis by Notch: evidence for multiple pathways. J Cell Physiol 2009;218:84–93.
29. ENCODE Project Consortium. An integrated encyclopedia of DNA elements in the human genome. Nature 2012;489:57–74.
30. Creyghton MP, Cheng AW, Welstead GG, et al. Histone H3K27ac separates active from poised enhancers and predicts developmental state. Proc Natl Acad Sci U S A 2010;107:21931–21936.
31. Fears CY, Grammer JR, Stewart JE Jr, et al. Low-density lipoprotein receptor-related protein contributes to the antiangiogenic activity of thrombospondin-2 in a murine glioma model. Cancer Res 2005;65:9338–9346.
32. Volpert OV, Tolsma SS, Pellerin S, et al. Inhibition of angiogenesis by thrombospondin-2. Biochem Biophys Res Commun 1995;217:326–332.
33. Tian W, Kyriakides TR. Matrix metalloproteinase-9 deficiency leads to prolonged foreign body response in the brain associated with increased IL-1beta levels and leakage of the blood-brain barrier. Matrix Biol 2009;28:148–159.
34. Reinecke H, Robey TE, Mignone JL, et al. Lack of thrombospondin-2 reduces fibrosis and increases vascularity around cardiac cell grafts. Cardiovasc Pathol 2013;22:91–95.
35. Taylor DK, Meganck JA, Terkhorn S, et al. Thrombospondin-2 influences the proportion of cartilage and bone during fracture healing. J Bone Miner Res 2009; 24:1043–1054.
36. Kyriakides TR, Maclauchlan S. The role of thrombospondins in wound healing, ischemia, and the foreign body reaction. J Cell Commun Signal 2009;3:215–225.
37. Iruela-Arispe ML, Liska DJ, Sage EH, et al. Differential expression of thrombospondin 1, 2, and 3 during murine development. Dev Dyn 1993;197:40–56.
38. Thakurdas SM, Lopez MF, Kakuda S, et al. Jagged1 heterozygosity in mice results in a congenital cholangiopathy which is reversed by concomitant deletion of one copy of Poglut1 (Rumi). Hepatology 2016;63:550–565.
39. Krady MM, Zeng J, Yu J, et al. Thrombospondin-2 modulates extracellular matrix remodeling during physiological angiogenesis. Am J Pathol 2008;173:879–891.
40. Zhang XJ, Wei CY, Li WB, et al. Association between single nucleotide polymorphisms in thrombospondins genes and coronary artery disease: a meta-analysis. Thromb Res 2015;136:45–51.
41. Yamada Y, Matsui K, Takeuchi I, et al. Association of genetic variants with coronary artery disease and ischemic stroke in a longitudinal population-based genetic epidemiological study. Biomed Rep 2015; 3:413–419.
42. Wang HQ, Jian T, Wang F, et al. Impact of thrombospondin-2 gene variations on the risk of thoracic aortic dissection in a Chinese Han population. Int J Clin Exp Med 2014;7:5796–5801.
43. Kimura Y, Izumiya Y, Hanatani S, et al. High serum levels of thrombospondin-2 correlate with poor prognosis of patients with heart failure with preserved ejection fraction. Heart Vessels 2016;31:52–59.
44. Dawson DW, Pearce SF, Zhong R, et al. CD36 mediates the In vitro inhibitory effects of thrombospondin-1 on endothelial cells. J Cell Biol 1997;138:707–717.

Received March 10, 2016. Accepted May 17, 2016.

Correspondence
Address correspondence to: Kathleen M. Loomes, MD, Division of Gastroenterology and Nutrition, Children's Hospital of Philadelphia, 902B Abramson Research Center, 3615 Civic Center Boulevard, Philadelphia, Pennsylvania 19104. e-mail: loomes@email.chop.edu; fax: (267) 426-7814.

Acknowledgments
The authors would like to thank the ChiLDReN Data Coordinating Center, and the principal investigators and clinical research coordinators at the ChiLDReN Centers for patient recruitment and sample acquisition. The authors also thank Dr Matthew Ryan for providing us with cDNA samples from laser capture microdissected mouse liver tissue. Finally, the authors would like to thank all of the patients and families who participated in our study.

Conflicts of interest
The authors disclose no conflicts.

Funding
This work was supported in part by the Childhood Liver Disease Research Network grant U01-DK062481 (K.M.L.); National Institutes of Health grants R01-DK081702-05 (N.B.S.) and R01-AR049682 (K.D.H.); National Institutes of Health training grant T32-HG000046 (E.A.T.); and VA Merit Award BX000375 (M.M.W.). The Childhood Liver Disease Research Network Data Coordinating Center is supported by U01 DK062456 from the National Institute of Diabetes and Digestive and Kidney Diseases (NIDDK). This work also was supported by the Fred and Suzanne Biesecker Liver Center at the Children's Hospital of Philadelphia.

Supplementary Table 1. Stratification of *JAG1* Mutation Type by Liver Disease Severity in GWAS Patients

Mutation type	Mild, %	Severe, %
Missense	21	14
Nonsense	31	31
Frameshift	31	38
Splice site alteration	7	9
Whole gene deletion	1	0
Partial gene deletion	3	3
Chromosome deletion	6	3
Partial gene duplication	0	2

Supplementary Table 2. List of Antibodies, Reagents, and Experimental Conditions for Immunohistochemistry and Immunofluorescence

Antibody	Species	Catalog number	Manufacturer	Working dilution
CD34	Rabbit	sc-9095	Santa Cruz Biotech, Dallas, TX	1:100
CK19	Rat	TROMAIII	University of Iowa, Iowa City, IA	1:75
GFP	Rabbit	ab6556	Abcam, Cambridge, MA	1:500[a]
GFP-FITC	Goat	Ab6662	Abcam	1:400
HNF4α	Goat	sc-6556	Santa Cruz Biotech	1:40
SMA	Rabbit	ab5694	Abcam	1:200
SM22α	Rabbit	ab14106	Abcam	1:100
Cy2 anti-rat	Donkey	712-225-153	Jackson ImmunoResearch, West Grove, PA	1:400
Dy488 anti-goat	Donkey	705-545-147	Jackson ImmunoResearch	1:400
Cy3 anti-rabbit	Donkey	711-165-152	Jackson ImmunoResearch	1:500
Biotinylated anti-rat IgG	Rabbit	BA-4001	Vector Laboratories, Burlingame, CA	

	Fix	Antigen retrieval	Block	Secondary antibody
CD34	3% Formaldehyde	-20°C Methanol	2% milk/5% BSA	Cy3-donkey anti-rabbit
CK19	3% Formaldehyde	0.25% Triton X-100	2% milk/5% BSA	Cy2-donkey anti-rat
GFP	3% Formaldehyde	0.25% Triton X-100	2% milk/5% BSA	Cy3-donkey anti-rabbit
GFP-FITC	3% Formaldehyde	0.25% Triton X-100	3% milk/10% BSA	N/A
HNF4α	3% Formaldehyde	0.25% Triton X-100	3% milk/10% BSA	Dy488-donkey anti-goat
SM22α	3% Formaldehyde	0.25% Triton X-100	3% milk/10% BSA	Cy3-donkey anti-rabbit

Other reagents	Catalog number	Manufacturer
Biotin	SP-2001	Vector Laboratories
Protein blocker	X0909	Dako, Carpenteria, CA
Avidin–biotin complex	PK-6100	Vector Laboratories
Antigen unmasking solution	H-3300	Vector Laboratories
SG substrate	SK-4700	Vector Laboratories
Nuclear Fast Red	H-3403	Vector Laboratories
Diaminobenzidine	K3468	Dako

FITC, fluorescein isothiocyanate; HNF4α, hepatocyte nuclear factor 4 α; SMA, smooth muscle actin; SM22, smooth muscle 22.
[a]The antibody concentration for adults was 1:500, the concentration for 1-week-old livers was 1:2250.

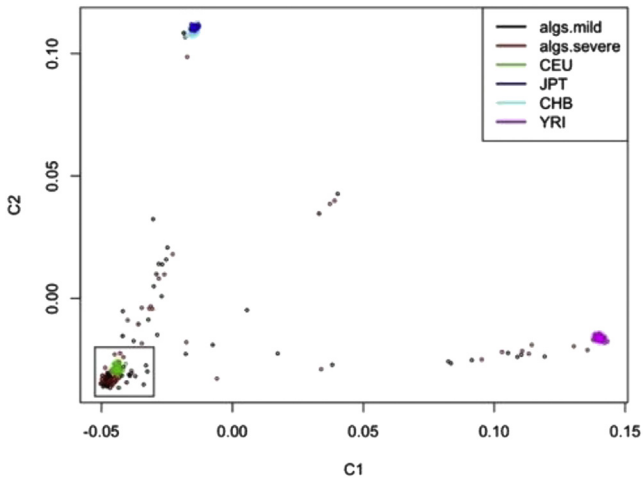

Supplementary Figure 1. Multidimensional scaling plot of ALGS patients with mild and severe liver disease. ALGS patients with mild and severe liver disease are plotted on top of the original 4 HapMap populations. We selected the individuals inside the *boxed region* as our cohort of patients with European ancestry. Utah residents with northern and western European ancestry (CEU), Japan in Tokyo (JPT), Han Chinese in Beijing (CHB), and Yoruba in Ibadan, Nigeria (YRI).

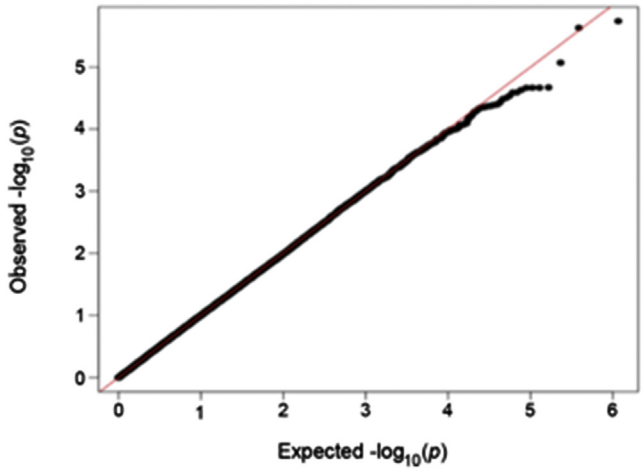

Supplemental Figure 2. Q-Q plot of association study. The observed *P* values from our variance component model (*black dots*) show a good fit to their expected distribution (*red line*) and therefore absence of inflation owing to population stratification or other forms of bias in the association test.